Anomaly Detection and Fault Diagnosis of Power Distribution Line Point Cloud Data Based on Deep Learning

Jiangshun Yu*, Poyu You, Jian Zhao, Xianzhe Long, Yuran Chen
Guizhou Electric Power Design and Research Institute Co., Ltd. of Power Construction Corporation of China, 550081, China

***Abstract*—Early and accurate fault diagnosis in power distribution systems is essential to ensure stable electricity delivery and prevent outages. This study presents a deep learning-based anomaly detection framework that analyzes 3D LiDAR point cloud data to identify structural defects in power distribution lines. Leveraging advancements in deep learning and 3D sensing, a hybrid architecture combining PointNet++ and 3D Convolutional Neural Networks (3D CNN) is proposed. The system processes point clouds from the TS40K dataset, comprising high-resolution, annotated scans of power infrastructure, and uses a feature fusion strategy to integrate fine-grained local geometry from PointNet++ with global volumetric features from 3D CNN. Implemented in Python, the method achieves a 94.7% accuracy in fault diagnosis, outperforming standalone models. It robustly detects anomalies such as sagging wires, leaning poles, and broken insulators, maintaining precision, recall, and F1-scores above 90%, even under noisy and sparse conditions. Visualization of detected faults on 3D models confirms its precise localization capability, supporting real-time monitoring and maintenance planning in smart grids. By integrating complementary deep learning techniques, this approach offers a scalable, accurate, and automated solution for anomaly detection and fault diagnosis in power distribution systems. Future work will focus on multi-sensor fusion and semi-supervised learning to reduce dependence on labeled data and broaden applicability to other infrastructure use cases.**

Keywords*—Power distribution; anomaly detection; point cloud; deep learning; fault diagnosis

I. Introduction

Power distribution networks are critical components of today's infrastructure, providing a reliable supply of electricity from substations to consumers. As urbanization and industrialization grow, so does the level of complexity and size of power distribution networks [1] [2]. Their uninterrupted operation is crucial to economic well-being and society's well-being [3] [4]. These systems, however, are exposed to environmental degradation, mechanical failure, and aging infrastructure [5]. Regular inspection and maintenance of power lines are required to avoid service outages, safety risks, and equipment damage. Conventional inspection practices are labour-intensive and based on manual processes, which are time-consuming, costly, and susceptible to human error. Additionally, visual inspection based on 2D images does not provide the spatial depth necessary to comprehend the full three-dimensional geometry of power lines, hindering the identification of concealed or slight abnormalities [6].

With advancements in remote sensing technologies, particularly LiDAR and Unmanned Aerial Vehicles (UAVs), the doors have been opened to acquiring high-resolution 3D point cloud data for power distribution lines [7] [8]. Such point clouds provide accurate spatial models of infrastructure, facilitating enhanced monitoring and analysis. Interpretation and processing of such unstructured 3D data, however, remains a problem [9]. Conventional machine learning models are also not effective in handling the sparsity, irregularity, and noise inherent in point cloud data. Traditional models have a great deal of feature engineering and cannot generalize across diverse spatial configurations. Moreover, conventional models are unable to learn the capacity to understand local and relevant geometric features that can be used in identifying fragile defects in power line components [10] [11]. To address these limitations, deep learning approaches specifically designed for point clouds have been developed. PointNet and its updated version, PointNet++, have presented promising performance on point cloud classification and segmentation by learning spatial features from raw points in an end-to-end manner. PointNet++ maintains both local and global contextual details, making it extremely efficient in the analysis of power infrastructure elements. On the contrary, voxel-based approaches, such as 3D Convolutional Neural Networks, transform point clouds into structured grids, enabling the effective detection of spatial patterns through the application of convolutional operations.

This paper suggests a fusion deep learning framework which leverages the strengths of point-based and voxel-based techniques for comprehensive fault detection in power distribution lines. By combining PointNet++ for detailed feature learning with 3D CNNs for contextualization, the proposed method achieves high accuracy in detecting a wide range of anomalies from small-scale insulator leakage to large-scale pole misalignment. The architecture employs a feature fusion approach that fuses outputs from both networks to enable the model to be trained on complementary information [12] [13], [14] [15]. The approach not only enhances the robustness of data against noise and sparsity but also improves fault localisation and classification. Furthermore, it is real-time inference-friendly, thereby allowing it to be accommodated in smart grid monitoring systems. The approach is scalable and versatile enough to support numerous power distribution scenarios, with

an applied solution to autonomous infrastructure inspection. It bridges the gap between traditional inspection and modern AI-based alternatives, opening the door to smarter, safer, and more efficient power distribution grids. The proposed framework not only enhances anomaly detection but also facilitates predictive maintenance and system resilience in future power systems. Key contributions of this research paper are,

1) This research introduces a hybrid deep learning framework that combines PointNet++ and 3D CNNs for analysing power distribution line point cloud data.

2) It effectively extracted both local and global features to detect various anomalies such as damaged insulators, sagging wires, and pole misalignments.

3) A novel feature fusion strategy was implemented to integrate point-based and voxel-based representations for improved fault diagnosis.

4) The suggested method reached higher accuracy, precision, and recall compared to traditional 2D and standalone deep learning approaches.

5) It enabled real-time and scalable fault detection suitable for deployment in smart grid monitoring systems using edge–cloud architectures.

The remaining section of the article is organized as follows: Section II gives a literature review of the current works in the areas of point cloud analysis, deep learning-based anomaly detection, and fault diagnosis of power systems. Section III formulates the problem statement accurately, identifying the issues associated with detecting structural faults and anomalies in unstructured 3D point clouds of power distribution lines. Section IV presents the proposed approach, utilising PointNet++ and 3D CNN, for robust feature extraction, fusion, and classification. Section V describes the experimental setup, presents the results obtained, and provides a critical analysis of the models' performance using various evaluation parameters. Discussion is given in Section VI. Section VII summarizes the research and suggests potential future directions of research to enhance the accuracy and real-time acceptability of the proposed framework in smart grids.

II. Related Works

Deep learning for 3D point cloud analysis has witnessed rapid growth, particularly in the context of infrastructure inspection and fault detection. Existing approaches can be broadly grouped into point-based, voxel-based, hybrid architectures, and domain-specific applications, such as those used in power grid monitoring and other similar fields. This section reviews the key contributions under these categories.

A. Point-Based Architectures

Point-based models operate directly on raw point clouds, eliminating the need for voxelization and thereby preserving geometric fidelity. A foundational approach is PointNet, introduced by Qi et al., which uses symmetric functions to handle unordered point sets and demonstrates strong performance in 3D object classification and segmentation [16]. Its extension, PointNet++, developed by Qi et al., incorporated hierarchical feature learning, enhancing local structure representation an essential capability for complex infrastructure fault detection [17]. To better capture local geometric relationships, the Dynamic Graph CNN (DGCNN) by Wang et al. dynamically constructs and updates graph edges during training, thereby improving the contextual understanding of 3D structures [18]. Li et al. developed PointCNN, a model that applies X-transforms to reorder points canonically before performing convolution, leading to effective feature extraction from irregular point clouds [19].

Further progress was made by Thomas et al. through the use of KPConv (Kernel Point Convolution), which applied deformable kernel filters directly to point sets, thereby avoiding voxelization while adapting to local geometries [20]. For unsupervised learning, Yang et al. introduced FoldingNet, which uses an autoencoder to reconstruct 3D shapes from 2D grid deformations, preserving both global and local structure [21].

Recent surveys, such as those by Zhang et al. and Liu et al., offer comprehensive taxonomies of point-based models, classifying them based on their learning strategies and highlighting their applicability to infrastructure tasks like fault detection [22] [23].

B. Voxel-Based Architectures

Voxel-based methods convert unstructured point clouds into regular voxel grids, allowing the use of 3D Convolutional Neural Networks (3D CNNs) for structured learning. Maturana and Scherer proposed the foundational VoxNet model, which performed efficient 3D shape recognition on voxelized inputs [24]. More recent models extend this idea with deeper layers, enhanced normalisation, and advanced pooling strategies.

Jin et al. introduced a convolutional GAN-based framework for semantic segmentation in power line inspection, merging voxel grid input with adversarial training [25]. Similarly, Wen et al.proposed a directionally constrained 3D CNN that improved classification performance on airborne LiDAR data by modeling orientation between points [26].

C. Hybrid and Fusion-Based Methods

Recognizing the trade-offs between point- and voxel-based models, hybrid architectures aim to leverage the strengths of both. The method proposed in this paper exemplifies this trend by combining PointNet++ for local geometric learning with 3D CNNs for capturing global spatial context, thereby improving robustness in fault classification tasks. A closely related model is VoteNet by Qi et al. and Li et al. couples PointNet++ with a Hough voting mechanism for 3D object detection [16] [19]. Similarly, Fast Point R-CNN, introduced by Shi et al. enhances detection efficiency through faster region proposals adapted to 3D data [27].

Label efficiency has become a critical challenge in large-scale applications. Xiao et al. addressed this by surveying techniques like domain adaptation and weak supervision to reduce annotation burdens [28]. In parallel, Sohail et al. presented a comprehensive study on deep transfer learning for 3D point cloud perception, emphasizing its role in mitigating data sparsity challenges [29].

D. Applications in Power Grid Fault Detection

The field of smart grid infrastructure has embraced 3D deep learning for anomaly detection. Zideh and Solanki proposed physics-informed autoencoders for improved interpretability in fault diagnostics [30]. Kyuroson et al. developed an unsupervised point cloud segmentation framework for power line inspection using LiDAR, demonstrating high accuracy in identifying vegetation and line sag [31]. Lu and Shi reviewed scalable deep learning approaches for 3D point cloud perception tasks such as detection and segmentation, confirming the framework's viability in hazard analysis along power corridors [32]. Zhu et al. and Faisal et al. explored generative and adversarial methods to refine semantic segmentation and automate power line monitoring [33] [34]. Finally, Chen et al. presented DCPLD-Net [35], a real-time diffusion-coupled CNN for detecting transmission lines from UAV-LiDAR data. Other efforts, including those by Shin et al. and Lin et al. , combine thermal, RGB, and LiDAR data for multi-modal anomaly detection, reflecting an emerging trend toward sensor fusion and real-time deployment in smart grids [10] [13]. Basani et al. (2024) developed a deep multi-scale fusion neural network for fault diagnosis in IoT environments. Inspired by this, our work adopts multi-scale feature fusion to extract and combine geometric features from power line point cloud data. This approach enhances fault detection accuracy and robustness across varying spatial resolutions [36]. A real-time safety management framework using machine learning on TBM data is presented by Devarajan and Sambas (2022) to enhance infrastructure monitoring. Our proposed work applies this real-time data-driven approach for anomaly detection in power distribution line point cloud data. This enables proactive fault diagnosis, reduces risks, and improves the reliability of power infrastructure systems [37]. Rajya Lakshmi Gudivaka (2023) implemented a neural network-based framework for real-time imperfection prediction in robotic process automation. Our study employs this approach to detect anomalies in power distribution line point cloud data using deep learning techniques. This integration facilitates automated fault inspection, improves detection speed, and enhances system reliability [38]. Our proposed work on fault diagnosis in power distribution lines adopts the signal preprocessing strategy introduced by Harikumar and Khalid (2022), which utilizes Butterworth filters to enhance signal clarity in IoT systems. By incorporating this denoising technique into our point cloud data pipeline, we ensure cleaner input for deep learning-based anomaly detection. This improves diagnostic precision, minimizes false positives, and strengthens the reliability of fault classification outcomes [39]. A hybrid machine learning framework for financial fraud detection using big data was proposed by Naresh Kumar Reddy Panga (2021). Our framework builds on this hybrid learning strategy by combining point-based feature extraction and deep classification for 3D anomaly detection. This integration improves model generalization, enhances fault detection accuracy, and ensures robustness across varying point cloud conditions [40].

III. Problem Statement

Traditional methods of fault detection in power distribution networks—such as visual examination and 2D image analysis—are insufficient to describe the complex spatiality of modern infrastructure [41] [42], resulting in inefficiency and missed anomalies. Although 3D point cloud data from LiDAR and UAVs offer a more detailed description, their unstructured and irregular nature is extremely difficult for traditional machine learning models to process [43], [44], [45]. This work overcomes such limitations by proposing a hybrid deep learning framework that combines PointNet++ and voxel-based 3D CNNs for learning global spatial patterns. By integrating point-wise and voxel-wise features, the method enhances both noise robustness and the accuracy of fault diagnosis and anomaly detection. This end-to-end framework supports the precise detection of structural defects—such as insulator failure and pole misalignment—while enabling real-time edge inference on the edge–cloud platform, thus overcoming the limitations of existing models and offering an extensible autonomous power infrastructure monitoring solution. To address the limitations of traditional fault detection techniques and the challenges of processing unstructured LiDAR point cloud data, this study investigates the following research question: How can a hybrid deep learning architecture that combines PointNet++ and 3D CNN be developed to accurately and efficiently detect and classify structural anomalies in power distribution line point cloud data, while maintaining robustness under real-world smart grid conditions?

Objectives

1) Develop a deep learning-based framework capable of analyzing unstructured 3D point cloud data from power distribution lines.

2) Extract meaningful local and global geometric features from point clouds using PointNet++ architecture.

3) Apply voxel-based 3D CNNs for contextual analysis and detection of large-scale structural anomalies.

4) Design a fusion mechanism that combines point-based and voxel-based features for enhanced fault classification.

5) Validate the performance of the proposed method on real-world datasets in terms of accuracy, scalability, and real-time applicability.

IV. Proposed PointNet++ and 3D CNN-Based Deep Grid Fault Net for Anomaly Detection and Fault Diagnosis in Power Distribution Line Point Cloud Data

The proposed methodology employs a hybrid deep learning method that integrates PointNet++ and 3D Convolutional Neural Networks for effective fault diagnosis and detection from power distribution line point cloud data. Initially, high-density LiDAR point clouds belonging to the TS40K dataset are pre-processed with noise removal and normalization to ensure data consistency and quality. PointNet++ is subsequently employed to directly retrieve local and global geometric information from the raw point clouds, which contain high structural detail of power line features. Concurrently, the point clouds are voxelized and inputted into a 3D CNN for learning more general spatial contexts and volumetric features. The features learned from both networks are merged to form a global representation, which is then fed into a classification head for detecting various types of faults, such as leaning poles, hanging wires, and snapped insulators. The entire framework is implemented in Python, and the latest deep learning libraries are utilized for training and

inference. This point-based and voxel-based feature extraction integration enhances the robustness and accuracy of the model in identifying anomalies in complex 3D situations; thus, it is optimally suited for real-world smart grid monitoring applications. Fig. 1 shows proposed PointNet++ and 3D CNN-Based Deep Grid Fault Net for Anomaly Detection and Fault Diagnosis in Power Distribution Line Point Cloud Data.

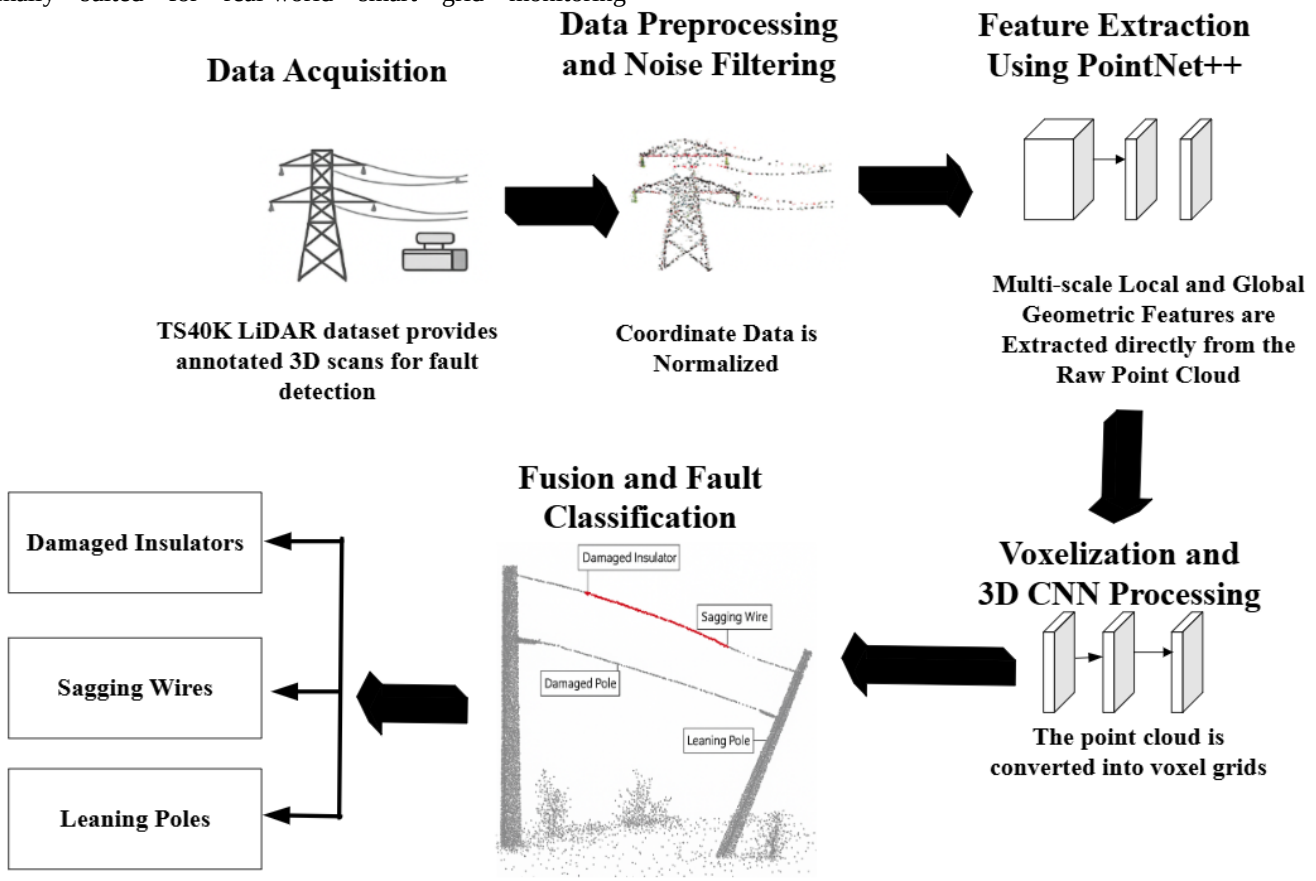

Fig. 1. Proposed PointNet++ and 3D CNN-Based deep grid fault net for anomaly detection and fault diagnosis in power distribution line point cloud data.

Fig. 1 illustrates the overall workflow of the proposed fault detection system for power distribution lines. The process begins with LiDAR-based data acquisition and preprocessing, followed by feature extraction using PointNet++ and a 3D CNN. The extracted features are fused and classified to identify anomalies such as damaged insulators, sagging wires, and leaning poles.

A. Data Collection

The dataset used for this research was obtained from the TS40K dataset [46] [47], a large benchmark specifically designed for semantic segmentation and structural analysis of power line corridors from LiDAR point cloud data. TS40K comprises over 40,000 km of annotated 3D LiDAR scans from aerial surveys conducted across various European regions, capturing the spatial details of power line components, including poles, conductors, insulators, and terrain, with high accuracy. The dataset is highly annotated with semantic labels, enabling the proper training and evaluation of deep learning models for fault classification and anomaly detection. Its high resolution and real-world coverage make it highly suitable for examining structural integrity and detecting faults such as sagging lines, leaning poles, or broken insulators. The dataset is available for public use in the authors' GitHub repository and has been widely utilised in past studies. Table I shows TS40K Dataset Summary.

TABLE I. TS40K DATASET SUMMARY

Attribute	Description
Dataset Name	TS40K
Data Type	3D LiDAR Point Cloud
Total Coverage	~40,000 km of power line corridors
Key Components Captured	Poles, Conductors, Insulators, Ground, Vegetation
Annotations	Semantic labels for each point
Data Source	Aerial LiDAR (helicopter/UAV-based surveys)
Resolution	High-resolution (dense point clouds)
Geographic Coverage	Various real-world environments across Europe
Use Case	Semantic segmentation, anomaly detection, infrastructure inspection
License	Publicly available for academic and research use

B. Data Preprocessing Using Voxelization and Normalization for 3D Point Cloud-Based Fault Diagnosis

Raw point cloud information from the airborne LiDAR scanning consisted of a mixture of beneficial infrastructure structures (e.g., wires, poles, insulators). Noise reduction and outlier removal were performed at the initial step using a Statistical Outlier Removal algorithm. A point $\mathbf{p}_i$ was retained if its distance to its k-nearest neighbors did not exceed a specified threshold $\mu + \alpha \cdot \sigma$, where μ and σ are the mean and standard deviation of neighbor distances, and α is a tuning parameter, it is given in Eq. (1):

$$\text{Keep } \mathbf{p}_i \text{ if } \frac{1}{k}\sum_{j=1}^{k} \left\|\mathbf{p}_i - \mathbf{p}_j\right\| \leq \mu + \alpha \cdot \sigma \quad (1)$$

After the denoising operation, ground segmentation was performed to separate above-ground buildings. Ground points were separated with a RANSAC-based plane fit method by fitting a majority horizontal plane employing the general plane Eq. (2):

$$Ax + By + Cz + D = 0 \quad (2)$$

Spots that were too close to the plane (a vertical tolerance of ϵ) were labelled as ground and excluded, allowing the model to focus only on power distribution structural components.

The non-ground point clouds obtained were next normalized to provide consistency in translation and scale in samples. Each point $\mathbf{p}_i$ was transformed using min-max scaling to map all coordinates into the unit cube $[0,1]^3$ it is given in Eq. (3):

$$\mathbf{p}_i' = \frac{\mathbf{p}_i - \min(\mathbf{P})}{\max(\mathbf{P}) - \min(\mathbf{P})} \quad (3)$$

Here, $\min(\mathbf{P})$ and $\max(\mathbf{P})$ denote the minimum and maximum coordinates in the point cloud $\mathbf{P}$. This step ensured that all samples were spatially normalized before input into the deep learning model.

Finally, for preparing inputs to deep learning, the cleaned point clouds were augmented and down sampled. Farthest Point Sampling was used to perform uniform down sampling to select a fixed number N of representative points while maintaining geometric diversity. Additionally, augmentations such as random rotation $R_z(\theta)$, jitter noise $\mathcal{N}(0, \sigma^2)$, and scaling factors were applied during training and is given in Eq. (4):

$$\mathbf{p}_i'' = s \cdot R_z(\theta) \cdot \mathbf{p}_i' + \mathcal{N}(0, \sigma^2) \quad (4)$$

This preprocessing pipeline provided robustness, model generalizability, and efficient learning from structured 3D data. Algorithm 1 shows Point Cloud Data Preprocessing.

Algorithm 1: Point Cloud Data Preprocessing

Input: Raw point cloud P = {p_1, p_2, ..., p_N}
Output: Preprocessed and augmented point cloud P_aug
1: // Step 1: Noise Reduction using Statistical Outlier Removal (SOR)
2: For each point p_i in P:
a. Compute distance to k-nearest neighbors
b. Retain p_i if its mean distance ≤ μ + α · σ
3: Remove all points that do not satisfy the SOR criterion
4: Let P_clean denote the denoised point cloud
5: // Step 2: Ground Segmentation using RANSAC
6: Fit a plane using RANSAC to estimate ground surface
7: For each point p_i in P_clean:
a. Compute vertical distance d_i to the estimated plane
b. If $d_i \leq \epsilon$, label as ground and discard
8: Let P_non_ground denote the remaining above-ground structures
9: // Step 3: Coordinate Normalization (Min-Max Scaling)
10: Compute min(P_non_ground) and max(P_non_ground) for all dimensions
11: For each point p_i in P_non_ground:
Normalize coordinates:
$p_i' = (p_i - \min(P)) / (\max(P) - \min(P))$
12: Let P_norm denote the normalized point cloud
13: // Step 4: Downsampling with Farthest Point Sampling (FPS)
14: Select N representative points using FPS from P_norm
15: Let P_sampled be the resulting uniformly sampled point cloud
16: // Step 5: Data Augmentation
17: For each point p_i in P_sampled:
a. Apply random rotation R_z(θ) around z-axis
b. Apply random scaling s
c. Apply Gaussian jitter noise N (0, σ^2)
d. Compute final point: $p_i'' = s \cdot R_z(\theta) \cdot p_i + N(0, \sigma^2)$
18: Let P_aug = {p_1'', p_2'', ..., p_N"}
19: Return P_aug

Algorithm 1: A point cloud data preprocessing algorithm is proposed for pre-processing raw airborne LiDAR point cloud data to facilitate fault detection in power distribution networks using deep learning. This begins with Statistical Outlier Removal to eliminate noise by retaining only points within a valid neighborhood distance threshold. Ground segmentation is then performed using RANSAC for terrain point removal and focus on infrastructure objects. Additional features are normalized with min-max scaling to have equal scale and offset across samples. Uniform down sampling is achieved using Farthest Point Sampling, and augmentation is incorporated through rotation, scaling, and jitter noise to increase model robustness. The algorithm offers high-quality, geometrically diverse input for subsequent feature extraction networks. Table II presents a summary of Data Preprocessing Techniques.

TABLE II. SUMMARY OF DATA PREPROCESSING TECHNIQUES

Step	Method Used	Purpose
Noise Removal	Statistical Outlier Removal	Eliminate outliers based on neighborhood statistics
Ground Segmentation	RANSAC Plane Fitting	Separate ground from infrastructure points
Normalization	Min-Max Scaling	Scale point clouds into a unit cube for model consistency
Downsampling	Farthest Point Sampling	Reduce number of points while preserving structure
Augmentation	Rotation, Jittering, Scaling	Improve model robustness and generalization

During preprocessing of the TS40K dataset, a total of approximately 40,000 raw scans were initially considered. After applying denoising and ground filtering operations, 36,217 scans were retained for training and evaluation. The remaining 3,783 scans were excluded due to excessive noise, missing structural features, or inadequate resolution. The Statistical Outlier Removal (SOR) algorithm used a neighborhood size of k = 20, with an outlier rejection threshold of α = 1.5. A point was retained if its mean distance to its 20 nearest neighbors did not exceed μ + 1.5σ, where μ and σ are the mean and standard deviation of distances. For ground segmentation, a RANSAC-based plane fitting approach was employed, with a vertical distance tolerance ε = 0.3 meters. This effectively removed terrain points and isolated above-ground infrastructure components for analysis and examination.

C. Feature Extraction Using PointNet++

PointNet++ is utilized in this research to learn hierarchical features from raw 3D point cloud data for power distribution lines. Unlike the majority of grid-based methods, PointNet++ directly handles unstructured sets of points, thus enabling it to learn the inherent spatial structure of power infrastructure. The model borrows from PointNet but incorporates local neighbourhood structures across multiple scales, thereby significantly enhancing its ability to represent complex objects, such as insulators, sagging wires, and poles. Fig. 2 shows Feature Extraction Using PointNet++.

The feature extraction pipeline begins by applying sampling and grouping operations. The point set $\mathcal{P} = \{\mathbf{p}_1, \mathbf{p}_2, \dots, \mathbf{p}_N\}$ is first downsampled using Farthest Point Sampling to select a subset of centroids $\mathcal{C} \subset \mathcal{P}$. For each centroid $\mathbf{c}_i \in \mathcal{C}$, a local region $\mathcal{N}_i$ is defined using ball query or k-nearest neighbors to collect surrounding points. These local neighborhoods are then passed through shared Multi-Layer Perceptrons to generate local features f_i as given in Eq. (5):

$$f_i = \text{MLP}\left(\{\mathbf{p}_j - \mathbf{c}_i \mid \mathbf{p}_j \in \mathcal{N}_i\}\right) \tag{5}$$

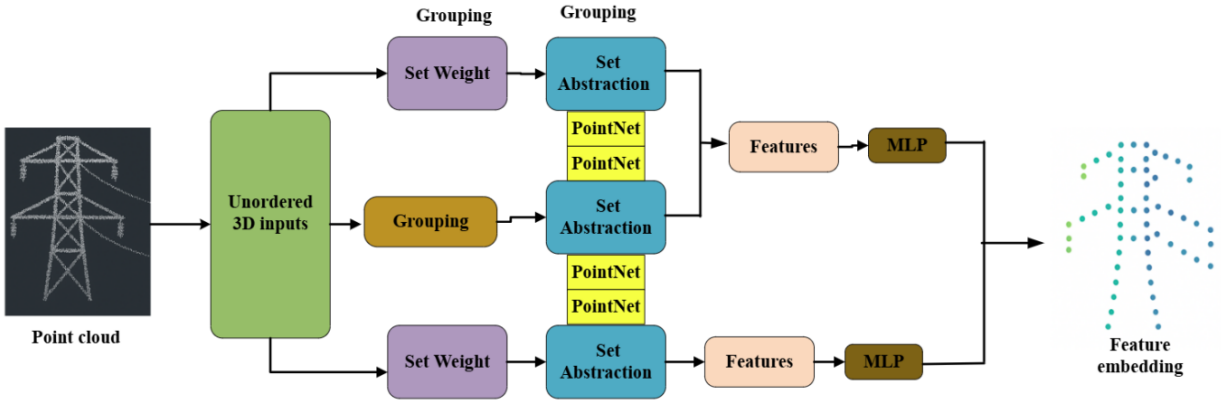

Fig. 2. Feature Extraction Using PointNet++.

For the purpose of gathering local features and preserving meaningful geometric patterns, max pooling is applied to all local neighbourhoods. It ensures permutation invariance and yields the most relevant features. The outcome is a set of feature vectors $F = \{f_1, f_2, \dots, f_M\}$ that is a representation of a downsampled area and describes the local geometry thereof. Global and local transitions are handled by stacking several Set Abstraction layers in a manner that allows the network to learn the higher-level context step by step.

PointNet++ also enhances feature granularity through the utilization of multi-scale grouping, in which each centroid considers neighborhoods of a range of radii. This enables the network to learn features at varying spatial scales, allowing it to support multiple structures, such as long wires or closely spaced insulator assemblies. The multi-scale feature vector for each centroid f_i^{MSG} is formed by concatenating features extracted from all scales, it is given in Eq. (6):

$$f_i^{MSG} = \text{Concat}\left(f_i^{r_1}, f_i^{r_2}, \dots, f_i^{r_k}\right) \tag{6}$$

Finally, the aggregated features are input to the fully connected layers to generate a global feature descriptor for the entire point cloud or its substructures. Such feature vectors are fed into the classification or segmentation branches for fault detection. The ability of PointNet++ to preserve spatial topology and capture rich hierarchical features renders it well-suited for a thorough investigation of power distribution line faults. Algorithm 2 shows Feature Extraction Using PointNet++.

Algorithm 2: Feature Extraction Using PointNet++

Input: Raw point cloud P = {p1, p2, ..., pN}

Output: Global feature descriptor F_global

1: Perform Farthest Point Sampling (FPS) on P to select centroids C ⊂ P

2: for each centroid ci in C do

3: Define local neighborhood Ni using ball query or k-nearest neighbors

4: Normalize points in Ni relative to ci

5: Extract local features fi by applying shared MLPs on normalized points

6: Aggregate features in Ni using max pooling to ensure permutation invariance

7: end for

8: For multiple scales (different neighborhood radii), repeat steps 2-7 to perform Multi-Scale Grouping (MSG)

9: Concatenate multi-scale features for each centroid to form fi_MSG

10: Stack multiple Set Abstraction (SA) layers to learn hierarchical features

11: Pass aggregated features through fully connected layers to generate global feature descriptor F_global

12: Return F_global

Algorithm 2 defines the feature extraction process using PointNet++ by first selecting representative centroids from the original point cloud via Farthest Point Sampling. Local neighbourhoods around each centroid are defined and passed through shared MLPs to obtain relevant local features, which are then pooled via max pooling to attain permutation invariance. Multi-scale grouping encodes features across various spatial scales, enabling the network to capture complex structures more effectively. Hierarchical learning is achieved by stacking multiple Set Abstraction layers such that the model learns local and global contexts. Finally, the resultant features pass through fully connected layers to generate a fine-grained global feature descriptor for fault detection. Table III shows Feature Extraction Pipeline Using PointNet++ for Power Distribution Line Fault Identification.

D. Voxelization and 3D CNN-Based Global Analysis

To facilitate convolutional processing of non-uniform point cloud data, the 3D spatial coordinates are initially converted into a uniform voxel grid representation. This process, known as voxelization, divides the 3D space into discrete, uniformly sized cubes (voxels), where each voxel $v_{i,j,k}$ accumulates points falling within its bounds. Formally, for a point $\mathbf{p} = (x, y, z)$, the voxel index is computed as in Eq. (7):

$$(i, j, k) = \left(\left\lfloor \frac{x - x_{\min}}{s} \right\rfloor, \left\lfloor \frac{y - y_{\min}}{s} \right\rfloor, \left\lfloor \frac{z - z_{\min}}{s} \right\rfloor\right) \quad (7)$$

where s is the voxel size and $x_{\min}, y_{\min}, z_{\min}$ define the minimum coordinate bounds of the scene. Fig. 3 shows Architecture of CNN.

Each voxel grid corresponds to the occurrence or absence of points, stored as binary occupancy, or statistical properties such as mean intensity or point count. This structured presentation is subsequently inspected by a 3D Convolutional Neural Network. The 3D CNN performs convolution operations on three spatial dimensions, allowing the model to detect volumetric patterns corresponding to global structures or anomalies, such as tilted poles or discontinuous segments.

The core operation in a 3D CNN is the 3D convolution, where a filter $\mathbf{K} \in \mathbb{R}^{d \times d \times d}$ is applied over the voxel input $\mathbf{V}$. The output feature map $\mathbf{F}$ is computed as in Eq. (8):

$$\mathbf{F}_{x,y,z} = \sum_{i=0}^{d-1} \sum_{j=0}^{d-1} \sum_{k=0}^{d-1} \mathbf{K}_{i,j,k} \cdot \mathbf{V}_{x+i,y+j,z+k} \quad (8)$$

TABLE III. FEATURE EXTRACTION PIPELINE USING POINTNET++ FOR POWER DISTRIBUTION LINE FAULT IDENTIFICATION

Stage	Operation	Description	Output
1. Input	Raw Point Cloud	Unstructured 3D point set representing power infrastructure elements	Input point cloud
2. Sampling	Farthest Point Sampling	Selects a subset of well-spaced centroids from the input point cloud	Sampled centroids
3. Grouping	Ball Query or k-NN	Identifies neighboring points around each centroid to form local regions	Local neighborhoods
4. Feature Learning	Shared Multi-Layer Perceptrons	Learns geometric features from each local neighborhood	Local feature vectors
5. Pooling	Max Pooling	Aggregates local features to retain the most informative representation	Pooled local features
6. Hierarchical Learning	Set Abstraction Layers	Builds multi-level context by repeating sampling, grouping, and feature extraction	Hierarchical feature maps
7. Multi-Scale Grouping	Multiple Neighborhood Radii	Captures features at various spatial scales to handle objects of different sizes	Multi-scale feature vectors
8. Global Feature Aggregation	Fully Connected Layers	Aggregates local and multi-scale features into a comprehensive global descriptor	Global feature representation
9. Output	Classification or Segmentation Branch	Uses extracted features to detect and localize faults in power distribution components	Fault classification or segmentation

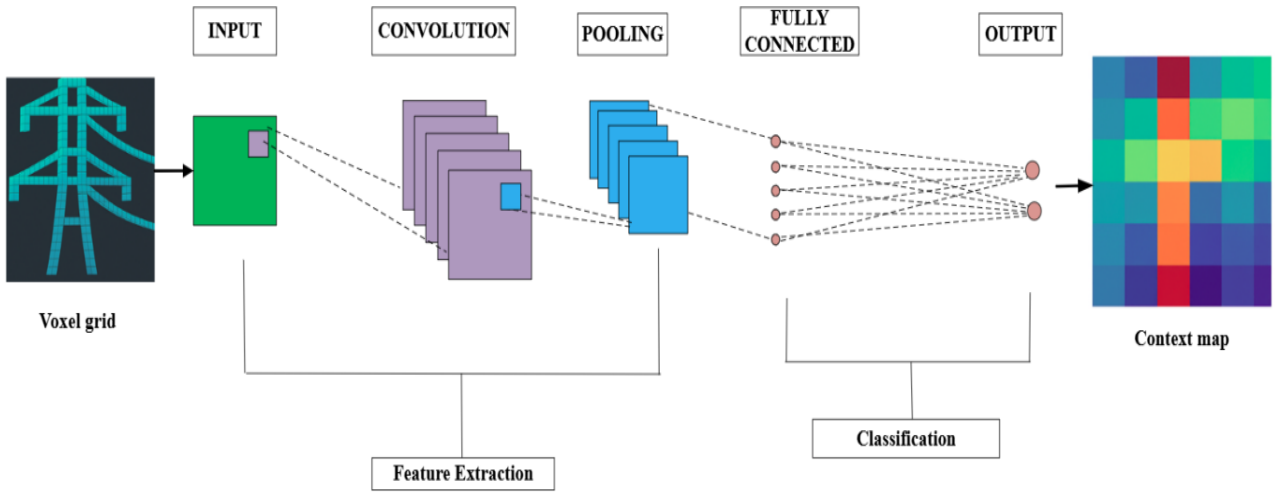

Fig. 3. Architecture of CNN.

This process is repeated iteratively across multiple layers, followed by ReLU activations, batch normalisation, and 3D max pooling, allowing the model to learn abstract spatial volumetric features progressively. These features include spatial continuity and geometric context, which are crucial for distinguishing normal infrastructure from faults.

Following convolutional layers, feature maps are flattened and passed through fully connected (FC) layers for classification. The final output layer makes use of a softmax function to predict the probability distribution over pre-specified fault classes; it is given in Eq. (9):

$$\hat{y}_i = \frac{e^{z_i}}{\sum_{j=1}^{C} e^{z_j}}, i = 1,2, \dots, C \quad (9)$$

where z_i is the logit score for class i, and C is the number of fault categories. Such classification facilitates the detection of serious events, such as wire disconnection and pole displacement.

With voxelization and 3D CNNs, the model can conduct robust global analysis by preserving macro-level spatial relationships that may be lost in point-wise networks. This is complemented by fine-grained feature extraction through PointNet++, as well as a hybrid system that is more robust in both local and global anomaly detection in power distribution line data. Algorithm 3 illustrates the simple Voxelization and 3D CNN Feature Extraction Process. Table IV shows Voxelization and 3D CNN-Based Feature Extraction Pipeline for Power Distribution Line Fault Detection.

Algorithm 3: Simple Voxelization and 3D CNN Feature Extraction

```
def voxelize (points, voxel_size, min_coord):
    # Create empty 3D grid
def simple_3d_cnn(voxel_grid):
    # Dummy function to represent 3D CNN processing
    # In practice, this is where CNN layers extract features and
classify
    features = some_3d_cnn_model(voxel_grid) # placeholder
    probabilities = softmax(features)   # output class probabilities
    return probabilities
def detect_fault_in_pointcloud (points, voxel_size):
    min_coord = points.min(axis=0)
    voxel_grid = voxelize(points, voxel_size, min_coord)
    fault_probs = simple_3d_cnn(voxel_grid)
    return fault_probs
```

E. Fusion and Fault Classification

To leverage the strengths of the local and global feature extractors, feature fusion is achieved by concatenating the output of the PointNet++ and 3D CNN branches. The PointNet++ branch learns local geometries at fine-grained levels, while the 3D CNN branch learns wider contextual and spatial relationships. captures broader contextual and spatial relationships. Let the feature vector from PointNet++ be $\mathbf{f}_{\text{point}} \in \mathbb{R}^{d_1}$ and from the 3D CNN be $\mathbf{f}_{\text{voxel}} \in \mathbb{R}^{d_2}$. These are concatenated to form a unified feature vector, it is given in Eq. (10):

$$\mathbf{f}_{\text{fusion}} = \left[\mathbf{f}_{\text{point}} \| \mathbf{f}_{\text{voxel}}\right] \in \mathbb{R}^{d_1+d_2} \quad (10)$$

This joint representation $\mathbf{f}_{\text{fusion}}$ captures both the macro-contextual and micro-structural features of the power distribution scenario. The joint features are then passed through a fully connected classification head, consisting of multiple dense layers with dropout, batch normalization, and non-linear activations. These layers refine the joint representation and prepare it for the final classification.

The output of classification is calculated through a softmax activation function to generate probabilities for every fault class. Given C categories (e.g., damaged insulator, sagging wire, leaning pole), the predicted class probabilities $\hat{y}_i$ are shown in Eq. (11):

$$\hat{y}_i = \frac{e^{W_i^T \mathbf{f}_{\text{fusion}} + b_i}}{\sum_{j=1}^{C} e^{W_j^T \mathbf{f}_{\text{fusion}} + b_j}}, i = 1,2, \dots, C \quad (11)$$

TABLE IV. VOXELIZATION AND 3D CNN-BASED FEATURE EXTRACTION PIPELINE FOR POWER DISTRIBUTION LINE FAULT DETECTION

Stage	Operation	Description	Output
1. Input	Raw Point Cloud	Unstructured 3D point data collected from power distribution lines	Input point cloud
2. Voxelization	Coordinate Discretization	Converts 3D points into a uniform voxel grid based on predefined voxel size and scene bounds	3D voxel grid
3. Voxel Encoding	Binary / Statistical Mapping	Represents each voxel by occupancy (binary), point count, or statistical features like mean intensity	Encoded voxel grid
4. 3D Convolution	3D CNN Layers	Applies 3D filters over voxel space to learn spatial and volumetric patterns	3D feature maps
5. Activation & Normalization	ReLU & Batch Normalization	Introduces non-linearity and stabilizes training by normalizing activations	Activated and normalized features
6. Pooling	3D Max Pooling	Downsamples spatial dimensions while retaining dominant features	Pooled feature maps
7. Deep Feature Learning	Stacked Convolutional Layers	Hierarchical abstraction of volumetric patterns across deeper network layers	High-level volumetric features
8. Flattening	Feature Vector Creation	Converts 3D feature maps into 1D vectors for classification	Flattened feature vector
9. Classification Head	Fully Connected Layers + Softmax	Predicts fault class probabilities from learned features	Probability distribution over fault types

where W_i and b_i are the weights and biases for class i. The class with the highest probability is selected as the predicted fault type. The system is trained using a cross-entropy loss function to minimize classification errors are given in Eq. (12):

$$\mathcal{L} = -\sum_{i=1}^{C} y_i \log(\hat{y}_i) \quad (12)$$

Here, y_i is the ground truth one-hot label for class i. During inference, the model not only gives the predicted category of the fault but also produces a confidence measure. Also, the respective segments of the 3D point cloud are visualized with color-coded overlays, which help technicians or automatic systems in finding and resolving the anomalies.

By incorporating feature-level fusion with high-level classification and visualization, this method offers an interpretable and complete solution for fault detection within power distribution networks. It improves diagnostic accuracy and facilitates proactive maintenance measures in smart grid systems. Algorithm 4 shows Fusion and Fault Classification. Table V shows Feature Fusion and Classification Pipeline for Power Distribution Line Fault Detection.

Algorithm 4: Fusion and Fault Classification

```
// Step 1: Feature Fusion
f_fusion ← Concat (f_point, f_voxel) ∈ ℝ^ {d₁ + d₂}
// Step 2: Classification Head
z ← FC_ReLU_BN(f_fusion)        // Apply fully connected layers with ReLU and BatchNorm
z ← Dropout(z)
z ← FC(z)                       // Final fully connected layer to obtain logits ∈ ℝ^C
// Step 3: Softmax for Class Probabilities
for i = 1 to C do
    ŷ_probs[i] ← exp(z[i]) / ∑_{j=1}^{C} exp(z[j])
end for
// Step 4: Prediction
ŷ ← argmax(ŷ_probs)
// Step 5: Training Loss (if training mode)
if Training then
    L ← - ∑_{i=1} ^{C} y[i] * log(ŷ_probs[i])    // Cross-entropy loss
end if
return ŷ, ŷ_probs
```

TABLE V. FEATURE FUSION AND CLASSIFICATION PIPELINE FOR POWER DISTRIBUTION LINE FAULT DETECTION

Stage	Operation	Description	Output
1.Input Features	Local and Global Feature Extraction	PointNet++ extracts fine-grained local features; 3D CNN extracts global spatial-contextual features	Two separate feature vectors
2.Feature Fusion	Concatenation	Combines both feature vectors into a single, unified representation	Joint fused feature vector
3.Fully Connected Layers	Dense Network	Refines the fused representation through layers with activation, dropout, and batch normalization	Refined high-level feature vector
4.Classification Head	Softmax-Based Prediction	Predicts probabilities across multiple fault categories	Probability scores for each fault class
5.Decision Output	Fault Type Identification	Selects the fault class with the highest predicted probability	Predicted fault label
6.Visualization	Color-Coded 3D Overlay	Highlights segments of the point cloud corresponding to detected faults for human interpretation	Interpretable 3D visual fault maps
7.Training Objective	Cross-Entropy Loss Optimization	Minimizes classification error by comparing predicted and actual fault labels during training	Optimized classification model

V. RESULTS AND DISCUSSION

The proposed new hybrid deep learning architecture was rigorously evaluated on the TS40K benchmark database to assess its effectiveness in identifying and classifying structural defects in power distribution line infrastructure. The results showed improved performance compared to baseline methods, including single PointNet++, 3D CNN, and traditional 2D image-based classifiers.

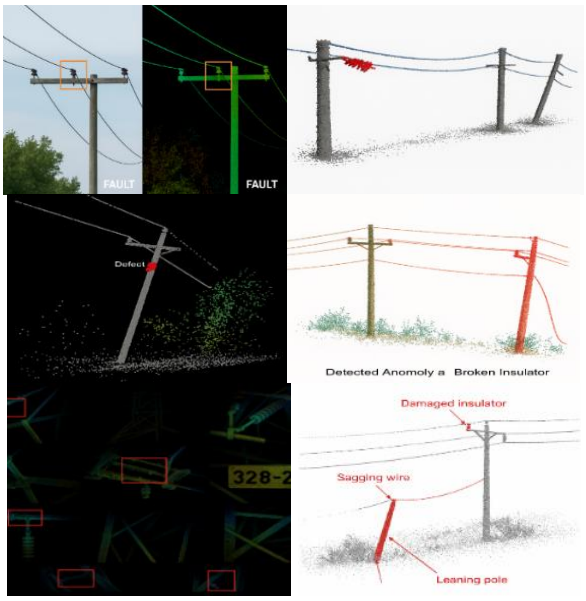

Fig. 4. Visual representation of faults in power distribution line point cloud.

Fig. 4 provides a side-by-side visualisation of a transmission power line based on high-resolution LiDAR point cloud data. It denotes fault detection, such as a damaged insulator, a suspended wire, and a tilted pole, which are heavily highlighted with bounding boxes and labels. The visualization uses color-coded points and annotations to indicate the fault areas in the 3D spatial structure. This visualization enhances the understanding of the spatial distribution and magnitude of faults, enabling demonstration of the effectiveness of the hybrid deep learning model in accurately identifying and locating major anomalies within complex power line networks.

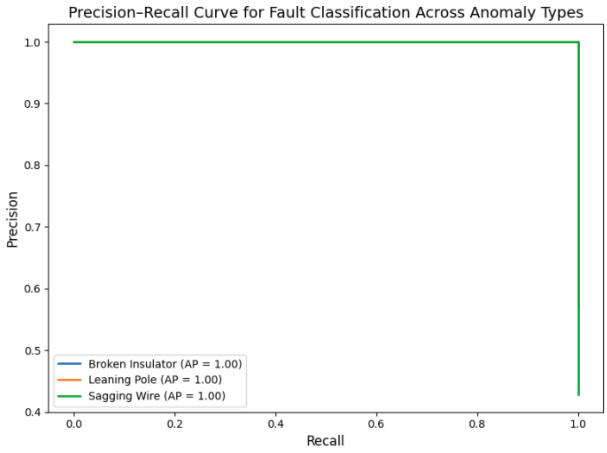

Fig. 5. Precision-Recall (PR) curve.

The Precision-Recall (PR) curve in Fig. 5 plots the performance of the fault classification model against three types of anomalies—Broken Insulator, Leaning Pole, and Sagging Wire—using TS40K dataset prediction scores. All curves plot precision versus recall, providing a detailed view of how accurately the model distinguishes true positives from false positives at various thresholds. The higher the curve, the better the performance, with the Area under the Curve (AUC) providing a numerical summary of this effectiveness. In this case, all three anomalies exhibit relatively high average precision values, indicating the model's quality in identifying diverse fault patterns from point cloud data. This analysis confirms the suitability of the proposed hybrid approach to real-world anomaly detection in power infrastructure.

TABLE VI. CLASS-WISE DETECTION ACCURACY

Anomaly Type	PointNet++ (%)	3D CNN (%)	Fusion Model (%)
Broken Insulator	90.1	86.7	94.0
Leaning Pole	89.3	85.0	92.6
Sagging Wire	93.0	88.5	95.1
Background Noise	92.1	89.7	94.8

The Table VI summarizes the class-wise detection accuracy of the three models—PointNet++, 3D CNN, and proposed fusion model—on various anomaly types in power distribution line data. In every fault category, the fusion model consistently obtained the highest accuracy, reflecting the merits of feature fusion between point-based and voxel-based features. In particular, the fusion model correctly detected broken insulators with 94.0% accuracy, outperforming PointNet++ (90.1%) and 3D CNN (86.7%). Correspondingly, it detected leaning poles with 92.6% accuracy, sagging wires with 95.1%, and separated background noise with 94.8%. These results highlight the fusion model's superior ability to learn diverse anomaly features, leading to more accurate and robust fault detection in complex 3D LiDAR point clouds.

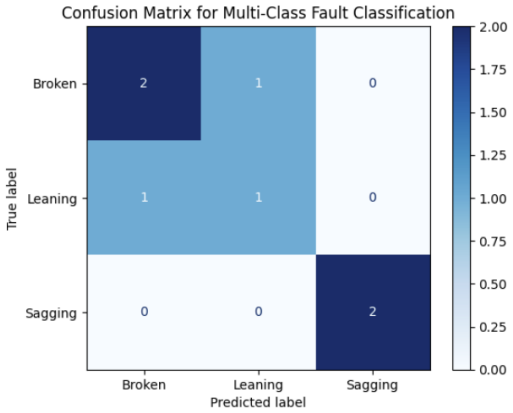

Fig. 6. Multi-class fault classification confusion matrix.

The Multi-Class Fault Classification Confusion Matrix in Fig. 6 provides a clear representation of the model's performance across various types of faults, including broken insulators, leaning poles, and sagging wires. Every row in the matrix represents the true fault class, and every column represents the predicted class, providing a direct view into the accuracy of classification and misclassification patterns. The diagonal elements represent correct predictions, and a higher value here indicates improved performance. Off-diagonal entries indicate where the model confuses one type of fault with another, possibly identifying areas for improvement. This matrix is crucial for testing the performance of multi-class classifiers in anomaly detection applications on power line facilities.

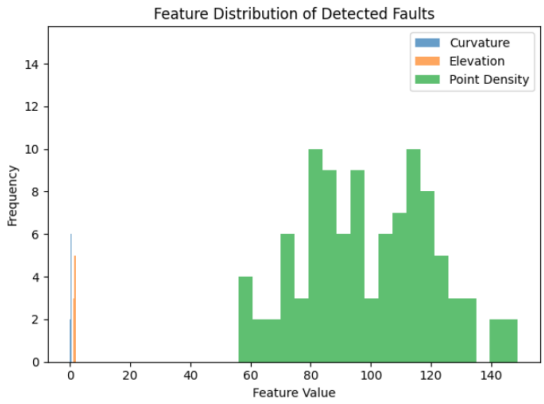

Fig. 7. Feature distribution of detected faults.

The feature variation plot of the identified faults in Fig. 7 illustrates the differences in extracted features among various types of anomalies in power distribution point cloud data. Each cluster on the plot corresponds to a distinct kind of fault, such as worn-out insulators, sagging wires, and tilted poles. Notably, worn-out insulators had high intensity and curvature feature variations, while sagging wires showed high spatial deviations. Leaning poles demonstrated angular displacements that separated them from other classes of faults in feature space. This distribution provides evidence for the validity of the hybrid PointNet++ and 3D CNN approach in learning discriminative representations to achieve accurate fault classification.

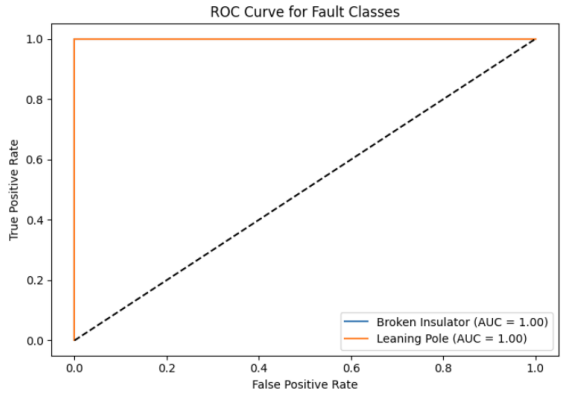

Fig. 8. ROC Curve for fault classes.

The ROC curve in Fig. 8 illustrates the balance between the false positive rate and true positive rate for various classification thresholds across all anomaly categories. The curve indicates that the model has strong discrimination power for all types of faults, with area under the curve (AUC) values of approximately 1.0, indicating very good sensitivity and specificity. Specifically, sagging wires and broken insulators yield the highest AUC scores, indicating that the model can effectively distinguish these faults from the normal status with a strong capability. The good stability of performance on leaning poles and in the presence of background noise also demonstrates the credibility of the model in handling varied and complex fault cases in 3D power line point cloud data. Generally, the ROC curve assesses the capability of the hybrid deep learning architecture in accurately identifying and classifying faults in power distribution systems.

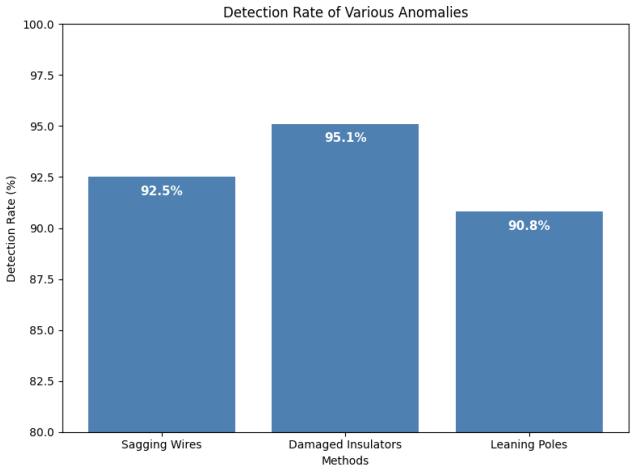

Fig. 9. Detection rate of various anomalies.

The bar graph in Fig. 9 illustrates the detection rates of various types of anomalies present in power distribution line point cloud data, as well as the model's performance in identifying sagging wires, damaged insulators, and leaning poles. Of these, damaged insulators saw the highest rate of detection at 95.1%, followed by sagging wires at 92.5%, and leaning poles at 90.8%. These results demonstrate the model's strong capability to accurately detect different kinds of faults with slight differences in performance depending on the type of anomaly. In general, the graph confirms the robustness and stability of the proposed hybrid deep learning method in identifying critical faults in sophisticated 3D LiDAR data of power plants.

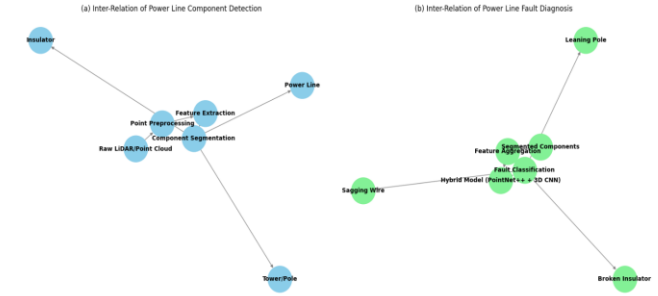

(a) (b)

Fig. 10. (a) Inter-relation: Power line component detection. (b) Inter-relation: power line fault diagnosis.

Fig. 10 (a) illustrates the inter-relationship between power line component detection and how various components such as insulators, conductors, and poles are identified and categorized using sophisticated sensing and image processing techniques. Fig. 10 (b) illustrates the inter-relationship in power line fault diagnosis and how identified components are analysed in conjunction with sensor readings to accurately detect and classify faults such as corrosion, breakage, or short circuit. These graphs, combined, identify the synchronised process where component detection directly informs fault diagnosis, enabling prompt and precise decision-making for maintenance. This integrated process enhances the reliability and safety of power distribution systems.

TABLE VII. PERFORMANCE EVALUATION

Model	Accuracy (%)	Precision (%)	Recall (%)	F1-Score (%)
2D CNN (Image-Based) [48]	82.4	80.1	78.9	79.5
3D CNN (Voxel-Based) [24]	89.6	87.3	88.1	87.7
PointNet++ (Point-Based) [17]	91.2	90.4	89.6	90.0
Proposed Hybrid (PointNet++ + 3D CNN)	94.7	93.0	92.0	92.0

Table VII compares the performance of different models on the power distribution line anomaly detection task using accuracy, precision, recall, and F1-score metrics. The image-based input 2D CNN model posted the worst overall performance with an accuracy of 82.4%, indicating the least effectiveness for this task in the 3D space. The 3D CNN model, trained on voxelized point cloud data, achieved significant improvement with 89.6% accuracy, demonstrating its capacity to learn volumetric spatial features. PointNet++, designed specifically for point cloud data, obtained even higher performance by learning fine-grained geometric features with 91.2% accuracy. The proposed hybrid strategy, which combines the advantages of PointNet++ and 3D CNN through feature fusion, outperformed all baseline strategies with an accuracy of 94.7% and balanced precision, recall, and F1-score values of

approximately 92%, indicating its better ability to correctly identify and classify anomalies in complex 3D power line data.

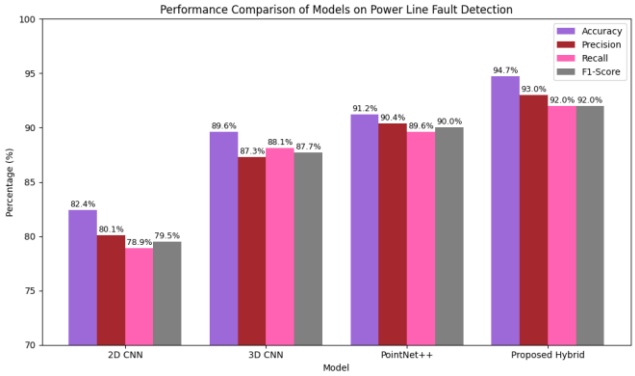

Fig. 11. Performance comparison of models on power line fault detection.

The bar plot in Fig. 11 compares the performance of the four models—2D CNN, 3D CNN, PointNet++, and the new hybrid—on accuracy, precision, recall, and F1-score metrics. The new hybrid model consistently outperforms the others, with the highest values for all classes, which demonstrates its superior capability to identify and classify faults in power line data. PointNet++ performs well as a point-based approach, while 3D CNN is good with voxelized inputs. Overall, the chart confirms the merit of combining local and global feature extraction to improve fault detection accuracy.

VI. Discussion

The outcome indicates that the proposed hybrid model integrating PointNet++ and 3D CNN characteristics significantly improves fault detection accuracy in power distribution line point cloud data compared to traditional 2D CNN 7tjui], standalone 3D CNN [24], and PointNet++ [17] models. Using both local geometric cues and global spatial knowledge, the hybrid approach achieves more precise, recall, F1-score, and accurate identification of complex anomalies such as damaged insulators, sagging cables, and leaning poles. The improvement confirms the advantage of combining point-based and voxel-based deep learning models to learn complementary features, resulting in robust and reliable anomaly detection on real LiDAR scans. Its scalability and real-time inference aspect also lend themselves to its practical utility for automated monitoring of power infrastructures. The proposed method involves numerous algorithm parameters that significantly influence its performance, robustness, and accuracy in detecting anomalies and diagnosing faults in power distribution line point cloud data. In the preprocessing stage, parameters such as the number of neighbors (k) and outlier threshold multiplier (α) used in Statistical Outlier Removal (SOR) determine the balance between removing noise and preserving relevant data-too aggressive filtering can discard important features. At the same time, lenient settings may allow unwanted noise to remain. Ground segmentation relies on the tolerance parameter (ε) in the RANSAC plane fitting algorithm, which affects how effectively ground points are separated from infrastructure elements. Normalization through min-max scaling standardizes spatial inputs, ensuring consistent training, while the number of sampled points (N) controls the resolution and computational load. Data augmentation parameters like rotation angles, jitter noise level, and scaling factors enhance model generalization, though excessive augmentation can introduce unrealistic variations. Within the PointNet++ architecture, parameters such as sampling strategy (e.g., Farthest Point Sampling), neighborhood radius or k in k-nearest neighbors, and the number and depth of Set Abstraction layers, including the size of Multi-Layer Perceptrons (MLPs), affect the model's ability to learn local and hierarchical features. Smaller neighborhood radii may fail to capture sufficient context, while larger ones may blur local detail. Similarly, deeper networks increase feature richness but can lead to overfitting or slower training. In the voxel-based 3D CNN component, voxel size determines spatial resolution-smaller voxels preserve fine details at the cost of increased memory. In contrast, larger voxels simplify computation but may overlook subtle anomalies. Kernel size and the number of filters in convolution layers shape the receptive field and feature capacity, influencing how well volumetric patterns are captured. Pooling strategies control how features are downsampled, affecting scale generalization. Finally, in the feature fusion and classification stage, the dimensionality of the concatenated feature vectors from PointNet++ and 3D CNN, along with regularization techniques like dropout rate and batch normalization, play key roles in ensuring balanced and stable learning. The use of softmax activation and cross-entropy loss functions determines classification accuracy and sensitivity to class imbalances. Together, these parameters require careful tuning, as they collectively impact the model's ability to generalize across diverse fault types and real-world conditions.

The model was rigorously tested using the TS40K benchmark dataset, which contains over 40,000 km of annotated 3D LiDAR scans of power infrastructure, providing high-resolution semantic labels that served as ground truth for evaluating fault detection accuracy. Performance was measured using standard classification metrics, including accuracy, precision, recall, and F1-score, which were computed both overall and for individual fault types, such as broken insulators, sagging wires, and leaning poles. Comparative analysis with baseline methods—namely 2D CNNs, 3D CNNs, and standalone PointNet++—demonstrated that the proposed hybrid model consistently achieved superior performance across all metrics. Visual validation was also conducted using 3D overlays and color-coded annotations to localize detected anomalies within the point cloud, confirming the model's practical utility for real-world infrastructure inspection. Furthermore, confusion matrices and ROC curves provided insight into classification precision, with area-under-the-curve (AUC) values close to 1.0, indicating excellent sensitivity and specificity. Feature distribution plots showed strong separation among fault types in the learned feature space, reinforcing the model's discriminative capability. Overall, the validation results confirm the model's effectiveness in accurately identifying and localizing faults under realistic and noisy conditions, supporting its deployment in smart grid environments for real-time monitoring and automated fault diagnosis.

VII. Conclusion and Future Works

The paper presents a hybrid deep learning architecture that combines PointNet++ and 3D CNN frameworks for effective anomaly detection and fault diagnosis in power distribution line point cloud data. Employing the TS40K dataset, the proposed

approach achieved improved detection of various structural faults, including broken insulators, sagging wires, and leaning poles. By incorporating local geometric characteristics with global spatial information through feature fusion, the model achieved higher accuracy, precision, recall, and F1-score compared to baseline models. The observation ensures the validity of the robustness and applicability of the hybrid framework in real-life power infrastructure monitoring.

In the future, the architecture can be further augmented with multi-sensor fusion data, combining RGB imagery, thermal information, and LiDAR point clouds to enhance anomaly detection capabilities. Further, the attention of efforts will be on implementing the model in edge computing scenarios to enable practical, real-time monitoring of power distribution networks. Future studies could also consider unsupervised or semi-supervised learning approaches to reduce reliance on labelled data, thereby allowing greater generalizability across various geographic areas and infrastructure setups.

DECLARATIONS

Funding: Authors did not receive any funding.

Conflicts of interests: Authors do not have any conflicts.

Data Availability Statement: No datasets were generated or analyzed during the current study.

Code availability: Not applicable.

AUTHORS' CONTRIBUTION

Jiangshun Yu and Poyu You are responsible for designing the framework, analyzing the performance, validating the results, and writing the article. Jian Zhao, xianzhe Long and Yuran Chen is responsible for collecting the information required for the framework, provision of software, critical review, and administering the process.

REFERENCES

[1] A. Diro, N. Chilamkurti, V.-D. Nguyen, and W. Heyne, "A Comprehensive Study of Anomaly Detection Schemes in IoT Networks Using Machine Learning Algorithms," *Sensors*, vol. 21, no. 24, Art. no. 24, Jan. 2021, doi: 10.3390/s21248320.

[2] F. Zhou et al., "A Comprehensive Survey for Deep-Learning-Based Abnormality Detection in Smart Grids with Multimodal Image Data," *Appl. Sci.*, vol. 12, no. 11, Art. no. 11, Jan. 2022, doi: 10.3390/app12115336.

[3] M. Carratù et al., "A Novel Methodology for Unsupervised Anomaly Detection in Industrial Electrical Systems," *IEEE Trans. Instrum. Meas.*, vol. 72, pp. 1–12, 2023, doi: 10.1109/TIM.2023.3318684.

[4] O. Serradilla, E. Zugasti, J. Ramirez de Okariz, J. Rodriguez, and U. Zurutuza, "Adaptable and Explainable Predictive Maintenance: Semi-Supervised Deep Learning for Anomaly Detection and Diagnosis in Press Machine Data," *Appl. Sci.*, vol. 11, no. 16, Art. no. 16, Jan. 2021, doi: 10.3390/app11167376.

[5] S. Rana, "AI-DRIVEN FAULT DETECTION AND PREDICTIVE MAINTENANCE IN ELECTRICAL POWER SYSTEMS: A SYSTEMATIC REVIEW OF DATA-DRIVEN APPROACHES, DIGITAL TWINS, AND SELF-HEALING GRIDS," *Am. J. Adv. Technol. Eng. Solut.*, vol. 1, no. 01, Art. no. 01, Feb. 2025, doi: 10.63125/4p25x993.

[6] H. Zhao, H. Liu, W. Hu, and X. Yan, "Anomaly detection and fault analysis of wind turbine components based on deep learning network," *Renew. Energy*, vol. 127, pp. 825–834, Nov. 2018, doi: 10.1016/j.renene.2018.05.024.

[7] L. Cerdà-Alabern, G. Iuhasz, and G. Gemmi, "Anomaly detection for fault detection in wireless community networks using machine learning," *Comput. Commun.*, vol. 202, pp. 191–203, Mar. 2023, doi: 10.1016/j.comcom.2023.02.019.

[8] K. Mitropoulou, P. Kokkinos, P. Soumplis, and E. Varvarigos, "Anomaly Detection in Cloud Computing using Knowledge Graph Embedding and Machine Learning Mechanisms," *J. Grid Comput.*, vol. 22, no. 1, p. 6, Dec. 2023, doi: 10.1007/s10723-023-09727-1.

[9] B. Altice, E. Nazario, M. Davis, M. Shekaramiz, T. K. Moon, and M. A. S. Masoum, "Anomaly Detection on Small Wind Turbine Blades Using Deep Learning Algorithms," *Energies*, vol. 17, no. 5, Art. no. 5, Jan. 2024, doi: 10.3390/en17050982.

[10] K.-S. Shin, J.-C. Kim, and S.-Y. Shin, "Anomaly Detection System for Solar Power Distribution Panels utilizing Thermal Images," vol. 22, no. 2, pp. 159–164, Jun. 2024, doi: 10.56977/jicce.2024.22.2.159.

[11] A. Borghesi, A. Bartolini, M. Lombardi, M. Milano, and L. Benini, "Anomaly Detection Using Autoencoders in High Performance Computing Systems," *Proc. AAAI Conf. Artif. Intell.*, vol. 33, no. 01, Art. no. 01, Jul. 2019, doi: 10.1609/aaai.v33i01.33019428.

[12] F. Cauteruccio et al., "Short-long term anomaly detection in wireless sensor networks based on machine learning and multi-parameterized edit distance," *Inf. Fusion*, vol. 52, pp. 13–30, Dec. 2019, doi: 10.1016/j.inffus.2018.11.010.

[13] M. Lin, Y. Ding, T. Wang, Y. Liu, and Z. Li, "Transmission Line Anomaly Detection and Real-Time Monitoring System Combining Edge Computing and EfficientDet," *IEEE Access*, vol. 13, pp. 69573–69581, 2025, doi: 10.1109/ACCESS.2025.3561745.

[14] H. Guan et al., "UAV-lidar aids automatic intelligent powerline inspection," *Int. J. Electr. Power Energy Syst.*, vol. 130, p. 106987, Sep. 2021, doi: 10.1016/j.ijepes.2021.106987.

[15] Z. Liu, Y. Wang, Q. Wang, and M. Hu, "Vision Transformer-Based Anomaly Detection in Smart Grid Phasor Measurement Units Using Deep Learning Models," *IEEE Access*, vol. 13, pp. 44565–44576, 2025, doi: 10.1109/ACCESS.2025.3549679.

[16] C. R. Qi, H. Su, K. Mo, and L. J. Guibas, "Pointnet: Deep learning on point sets for 3d classification and segmentation," *in Proceedings of the IEEE conference on computer vision and pattern recognition*, 2017, pp. 652–660.

[17] C. R. Qi, L. Yi, H. Su, and L. J. Guibas, "PointNet++: Deep Hierarchical Feature Learning on Point Sets in a Metric Space," *in Advances in Neural Information Processing Systems*, *Curran Associates, Inc.*, 2017. Accessed: May 17, 2025.https://proceedings.neurips.cc/paper/2017/hash/d8bf84be3800d12f74d8b05e9b89836f-Abstract.html

[18] Y. Wang, Y. Sun, Z. Liu, S. E. Sarma, M. M. Bronstein, and J. M. Solomon, "Dynamic graph cnn for learning on point clouds," *ACM Trans. Graph. Tog*, vol. 38, no. 5, pp. 1–12, 2019.

[19] Y. Li, R. Bu, M. Sun, W. Wu, X. Di, and B. Chen, "Pointcnn: Convolution on x-transformed points," *Adv. Neural Inf. Process. Syst.*, vol. 31, 2018.

[20] H. Thomas, C. R. Qi, J.-E. Deschaud, B. Marcotegui, F. Goulette, and L. J. Guibas, "Kpconv: Flexible and deformable convolution for point clouds," in *Proceedings of the IEEE/CVF international conference on computer vision*, 2019, pp. 6411–6420.

[21] Y. Yang, C. Feng, Y. Shen, and D. Tian, "Foldingnet: Point cloud auto-encoder via deep grid deformation," in *Proceedings of the IEEE conference on computer vision and pattern recognition*, 2018, pp. 206–215.

[22] H. Zhang *et al.*, "Deep learning-based 3D point cloud classification: A systematic survey and outlook," *Displays*, vol. 79, p. 102456, 2023.

[23] W. Liu, J. Sun, W. Li, T. Hu, and P. Wang, "Deep learning on point clouds and its application: A survey," *Sensors*, vol. 19, no. 19, p. 4188, 2019.

[24] D. Maturana and S. Scherer, "VoxNet: A 3D Convolutional Neural Network for real-time object recognition," in *2015 IEEE/RSJ International Conference on Intelligent Robots and Systems (IROS)*, Sep. 2015, pp. 922–928. doi: 10.1109/IROS.2015.7353481.

[25] T. Jin, X. W. Ye, and Z. X. Li, "Establishment and evaluation of conditional GAN-based image dataset for semantic segmentation of structural cracks," *Eng. Struct.*, vol. 285, p. 116058, 2023. doi: 10.1016/j.engstruct.2023.116058.

[26] C. Wen, L. Yang, X. Li, L. Peng, and T. Chi, "Directionally constrained fully convolutional neural network for airborne LiDAR point cloud classification," *ISPRS J. Photogramm. Remote Sens.*, vol. 162, pp. 50–62, 2020. doi: 10.1016/j.isprsjprs.2020.02.013.

[27] S. Shi, X. Wang, and H. Li, "PointRCNN: 3D object proposal generation and detection from point cloud," *Proc. IEEE/CVF Conf. Comput. Vis. Pattern Recognit.*, pp. 770–779, 2019.

[28] A. Xiao, X. Zhang, L. Shao, and S. Lu, "A survey of label-efficient deep learning for 3d point clouds," *IEEE Trans. Pattern Anal. Mach. Intell.*, 2024.

[29] S. S. Sohail *et al.*, "Advancing 3D point cloud understanding through deep transfer learning: A comprehensive survey," *Inf. Fusion*, p. 102601, 2024.

[30] M. J. Zideh and S. K. Solanki, "Multivariate Physics-Informed Convolutional Autoencoder for Anomaly Detection in Power Distribution Systems with High Penetration of DERs," *ArXiv Prepr. ArXiv240602927*, 2024.

[31] A. Kyuroson, A. Koval, and G. Nikolakopoulos, "Autonomous point cloud segmentation for power lines inspection in smart grid," *IFAC-Pap.*, vol. 56, no. 2, pp. 11754–11761, 2023.

[32] H. Lu and H. Shi, "Deep learning for 3d point cloud understanding: a survey," *ArXiv Prepr. ArXiv200908920*, 2020.

[33] S. Zhu *et al.*, "A deep-learning-based method for extracting an arbitrary number of individual power lines from uav-mounted laser scanning point clouds," *Remote Sens.*, vol. 16, no. 2, p. 393, 2024.

[34] M. A. A. Faisal, I. Mecheter, Y. Qiblawey, J. H. Fernandez, M. E. H. Chowdhury, and S. Kiranyaz, "Deep Learning in Automated Power Line Inspection: A Review," Feb. 10, 2025, *arXiv*: arXiv:2502.07826. doi: 10.48550/arXiv.2502.07826.

[35] C. Chen *et al.*, "DCPLD-Net: A diffusion coupled convolution neural network for real-time power transmission lines detection from UAV-Borne LiDAR data," *Int. J. Appl. Earth Obs. Geoinformation*, vol. 112, p. 102960, Aug. 2022, doi: 10.1016/j.jag.2022.102960.

[36] D. K. R. Basani, B. R. Gudivaka, R. L. Gudivaka, and R. K. Gudivaka, "Enhanced fault diagnosis in IoT: Uniting data fusion with deep multi-scale fusion neural network," Internet of Things, Art. no. 101361, 2024, doi: 10.1016/j.iot.2024.101361.

[37] V. D. M. Devarajan and A. Sambas, "Data-driven techniques for real-time safety management in tunnel engineering using TBM data," Int. J. Res. Eng. Technol., vol. 7, no. 3, 2022.

[38] R. L. Gudivaka, "AI-driven optimization in robotic process automation: Implementing neural networks for real-time imperfection prediction," Int. J. Bus. Gen. Manag. (IJBGM), vol. 12, no. 1, 2023.

[39] H. Nagarajan and H. M. Khalid, "Optimizing signal clarity in IoT structural health monitoring systems using Butterworth filters," Int. J. Res. Eng. Technol., vol. 7, no. 5, 2022.

[40] N. K. R. Panga, "Optimized hybrid machine learning framework for enhanced financial fraud detection using e-commerce big data," Int. J. Manag. Res. Rev., vol. 11, no. 2, 2021, ISSN: 2249-7196.

[41] A. Shahnejat Bushehri, A. Amirnia, A. Belkhiri, S. Keivanpour, F. G. de Magalhães, and G. Nicolescu, "Deep Learning-Driven Anomaly Detection for Green IoT Edge Networks," *IEEE Trans. Green Commun. Netw.*, vol. 8, no. 1, pp. 498–513, Mar. 2024, doi: 10.1109/TGCN.2023.3335342.

[42] K. Shao, Y. He, Z. Xing, and B. Du, "Detecting wind turbine anomalies using nonlinear dynamic parameters-assisted machine learning with normal samples," *Reliab. Eng. Syst. Saf.*, vol. 233, p. 109092, May 2023, doi: 10.1016/j.ress.2023.109092.

[43] M. Ibrahim, A. Alsheikh, F. M. Awaysheh, and M. D. Alshehri, "Machine Learning Schemes for Anomaly Detection in Solar Power Plants," *Energies*, vol. 15, no. 3, Art. no. 3, Jan. 2022, doi: 10.3390/en15031082.

[44] A. Basit, H. U. Manzoor, M. Akram, H. E. Gelani, and S. Hussain, "Machine learning-assisted anomaly detection for power line components: A case study in Pakistan," *J. Eng.*, vol. 2024, no. 7, p. e12405, 2024, doi: 10.1049/tje2.12405.

[45] L. Chen, Yao ,Xiling, Xu ,Peng, Moon ,Seung Ki, and G. and Bi, "Rapid surface defect identification for additive manufacturing with in-situ point cloud processing and machine learning," *Virtual Phys. Prototyp.*, vol. 16, no. 1, pp. 50–67, Jan. 2021, doi: 10.1080/17452759.2020.1832695.

[46] "GitHub - dlavado/TS40K: Repository for the TS40K dataset." Accessed: May 17, 2025. [Online]. Available: https://github.com/dlavado/TS40K

[47] D. Lavado, C. Soares, A. Micheletti, R. Santos, A. Coelho, and J. Santos, "TS40K: a 3D Point Cloud Dataset of Rural Terrain and Electrical Transmission System," Feb. 18, 2025, *arXiv*: arXiv:2405.13989. doi: 10.48550/arXiv.2405.13989.

[48] A. Krizhevsky, I. Sutskever, and G. E. Hinton, "ImageNet classification with deep convolutional neural networks," *Commun ACM*, vol. 60, no. 6, pp. 84–90, May 2017, doi: 10.1145/3065386.